CONF-830942 -- 19

THE EFFECT OF PHOSPHORUS ON THE SWELLING AND PRECIPITATION BEHAVIOR OF AUSTENITIC STAINLESS STEELS DURING IRRADIATION*

EAL H. LEE, L. K. MANSUR, and A. F. ROWCLIFFE

Metals and Ceramics Division, Oak Ridge National Laboratory, Oak Ridge, Tennessee 37831

It has been observed that increasing the volume fraction of the needle-shaped iron phosphide phase in austenitic stainless steels tends to inhibit void swelling during neutron irradiation. An earlier analysis showed that this effect could not be accounted for in terms of enhanced point defect recombination at particle-matrix interfaces. The behavior of the iron phosphide phase has been further examined using dual ion beam irradiations. It was found that the particle-matrix interface serves as a site for the nucleation of a very fine dispersion of helium bubbles. It is thought that since a high number density of cavities lowers the number of helium atoms per cavity, the irradiation time for the cavities to accumulate the critical number of gas atoms for bias-driven growth is correspondingly increased. Although the phosphide phase nucleates rapidly, it eventually undergoes dissolution if either the G or Laves phase develops with increasing dose.

1. INTRODUCTION

Type 316 austenitic stainless steels are potential candidate alloys for breeder reactor and magnetic fusion energy (MFE) structural materials applications. Considerable effort has been devoted to designing radiation resistant alloys, mainly by modifying minor elemental components such as Si, Ti, Mo, B, P, etc. In the modified stainless steels various precipitates such as G, eta, Laves, γ', MC, and silicon rich phosphides form during irradiation. The swelling and creep behavior of these complex alloys is strongly influenced by the precipitate phases which form during irradiation. In general large precipitates are detrimental, since cavities associated with large particles grow more rapidly than cavities in the matrix. There is evidence that other precipitates such as γ', MC, and the phosphides suppress cavity swelling when their particle densities are very high. This work is part of a continuing assessment[1,2,3] of the effect of these precipitates on swelling. The alloys investigated here are phosphide-forming austenitic stainless steels. Significant insight is gained regarding the role of precipitates.

2. EXPERIMENTAL

The approximate base composition (wt %) of the alloys used in this study is Fe-16Cr-14Ni-2.5Mo-2Mn-0.2Ti-0.04C. Two different levels of silicon and phosphorous have been studied: alloy A7 has 1.4 Si and 0.08 P, while alloy A27 has 0.7 Si and 0.04 P. Solution annealed (1100°C/0.25 h) specimen disks 3-mm diam by 0.35-mm thick were irradiated in EBR-II, and also in the ORNL dual-ion beam Van de Graaff facility. Alloy A7 was also prepared in the 20% cold worked condition. A dose of ~32 dpa (E > 0.1 MeV) was attained in EBR-II at 555°C. Doses of 50 and 90 dpa were attained at 675°C by employing simultaneous injection of 4 MeV $^{58}Ni^{++}$ and 0.2–0.4 MeV He^+ ions at a ratio of 0.4 appm He/dpa, which is comparable to the helium generation rate in EBR-II. Following irradiations, specimens were electrochemically

thinned to examine the damaged region. Details of the ion irradiation method and sample preparation techniques are described elsewhere.[4,5] A JEM 120CX electron microscope was used for general examination and a Philips EM400T equipped with a field emission gun was used for high resolution work. Quantitative measurements of cavity, precipitate, and dislocation parameters were evaluated from stereo pairs of TEM micrographs.

3. RESULTS

3.1. Neutron irradiation

Both alloys A7 and A27 irradiated at 555°C to a dose of ∼32 dpa (E > 0.1 MeV) in the fast reactor EBR-II have been examined by analytical transmission electron microscopy. Both the swelling and precipitate behavior differed substantially in the two alloys as shown in Figure 1. There is an inverse correlation between the extent of the swelling and the scale of the precipitation. The precipitate particles which developed were principally the needle shaped iron phosphide phase, Fe_2P, with additional very small amounts of Laves, G, eta, and MC particles. Information regarding the phase identification is described in detail in a previous publication.[6] The phosphide particles were rich in silicon and nickel, with the typical composition (wt %) of 16Si-5P-4S-19Cr-29Fe-27Ni. The principal effect of increasing the phosphorous and silicon concentrations was to increase the volume fraction of phosphide precipitates. In alloy A7 (Figure 1a) where the phosphorous and silicon concentrations are twice as high as in alloy A27 (Figure 1b), the precipitate number density is three times as high. The average size of the precipitates also increased by a factor of 1.5–2, mainly in the length along the <001> direction of the matrix. In alloy A7 swelling was totally suppressed as shown in Figure 1. Alloy A27, however, contained cavities with an average diameter of 35 nm and a number density of about $2 \times 10^{20}/m^3$, to give a swelling of 0.46%. Quantitative microstructural information for the two alloys is given in Table 1.
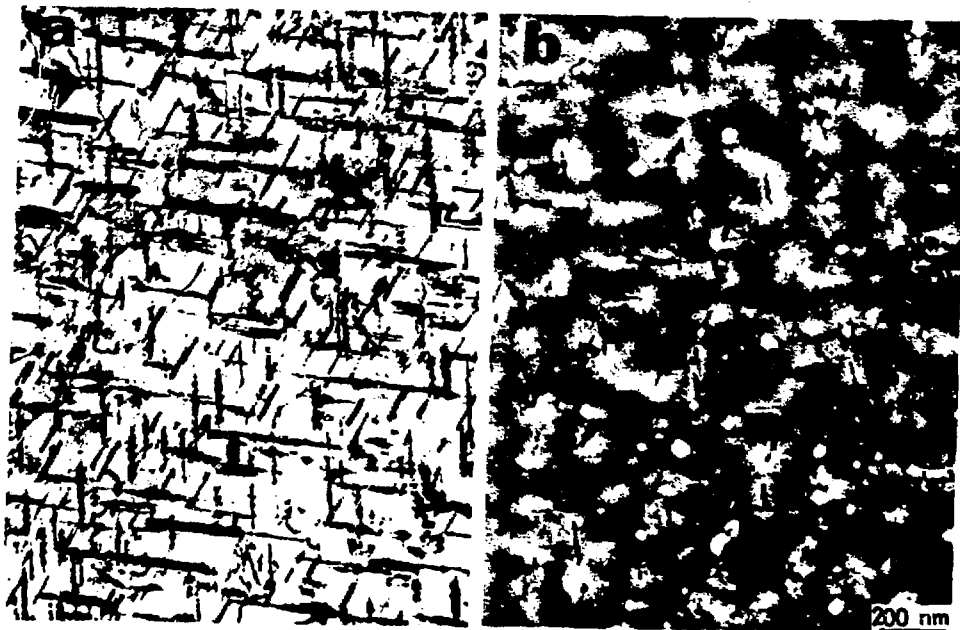

FIGURE 1
(a) Alloy A7 (1.4 Si, 0.08 P) and (b) alloy A27 (0.7 Si, 0.04 P) neutron irradiated to a dose of ∼32 dpa (E > 0.1 MeV) in EBR-II at 555°C.

Alloy	Dose (dpa)	Dislocation Density (m^{-2})	Average Cavity Diameter (nm)	Cavity Density (m^{-3})	Average ppt. Dimension (nm)	Precipitate Density (m^{-3})	He-atoms per Bubble, n_g (m^{-3})	n_g^*
A7	50(Ni++)	1.8×10^{14}	—	$\sim 1.5 \times 10^{22}$	230×15×7	6.2×10^{20d}	130	370
A7	90(Ni++)	—	—	—	—	—	230^b	
A7	32(n)	8×10^{13}	—	$\sim 1.8 \times 10^{21c}$	300×20×10	6×10^{20}	730	1210
A27	32(n)	3.1×10^{14}	35	$\sim 2.0 \times 10^{20}$	200×10×5	2×10^{20}	6500	3750

[a]Phosphide and G-phase.
[b]Used same microstructure as "50 dpa" to minimize precipitate dissolution effect.
[c]Estimated by taking same areal density of cavities on precipitate matrix interface as in neutron irradiated alloy
A27 times the ratio of interfacial area in alloy A7 to alloy A27.

3.2. Ion irradiation

Alloy A7 was irradiated at 675°C simultaneously with 4 MeV Ni++ ions and 0.2–0.4 MeV He+ ions with a 0.4 appm He/dpa injection ratio. Figure 2 shows the microstructures after 50 dpa (Figure 2a) and 90 dpa (Figure 2b). An ion irradiation temperature of 675°C was chosen since earlier work had shown that precipitation reactions in stainless steels occur rapidly at this temperature. After 50 dpa, the microstructure was dominated by the needle-shaped phosphide phase with some G-phase also present. The density of phosphide particles was $\sim 5 \times 10^{20}/m^3$ and that of the G phase was $\sim 1.2 \times 10^{20}/m^3$. Examination after 90 dpa however showed that the situation had reversed. Beyond 50 dpa, the phosphide phase apparently dissolved with a reduction in both the number and size of particles. At the same time, the volume fraction of coarse G-phase particles
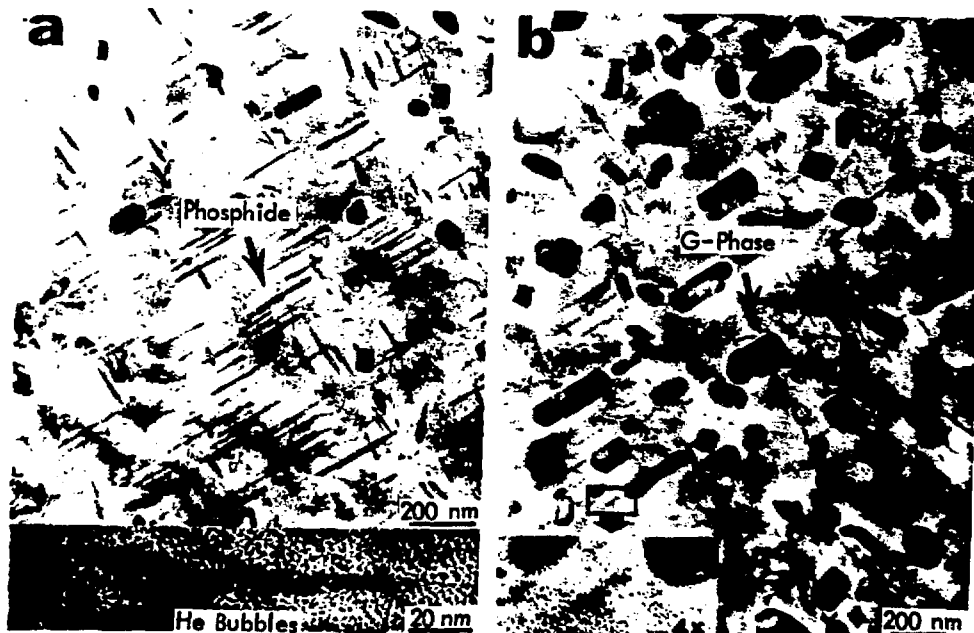

FIGURE 2
Alloy A7 irradiated to 4 MeV Ni-ions at 675°C with 0.4 appm He/dpa ratio: (a) 50 dpa and (b) 90 dpa.

increased without a substantial increase in number density. At both doses, a small volume fraction of MC phase was found, but Laves phase did not develop.

The specimens of SA alloy A7 irradiated to 90 dpa (Figures 3a,b) and of CW alloy A7 irradiated to 35 dpa (Figures 3c,d) were examined beyond the region of 4 MeV Ni ion damage. Phosphide particles could not be detected in either case. One of the SA alloy A7 specimens which had been irradiated to 50 dpa was subjected to a post-irradiation anneal of 16 hours at 675°C. Partial dissolution of the G and phosphide phases occurred, the degree of dissolution varying considerably from one region to another within the same grain. In regions where dissolution occurred, the phosphide and G phase precipitates were replaced by precipitation of fine MC particles.

Cavity swelling in alloy A7 was almost negligible up to 90 dpa with the occasional cavity occurring in association with a G phase particle. The unusual swelling resistance of this material prompted an investigation of the distribution of injected helium using high resolution electron microscopy. The inset portion of Figure 2a is a high resolution micrograph obtained using a Philips EM400T/FEG instrument. After 50 dpa, about 10-30 small helium bubbles were imaged at the particle-matrix interface of each phosphide precipitate examined. The bubble diameters were in the range 1-2 nm — too small to be imaged by conventional methods. It was estimated from high resolution micrographs that one helium bubble exists per 400 nm^2 of precipitate-matrix interface. The 90 dpa specimen was not of sufficient quality for high resolution work.
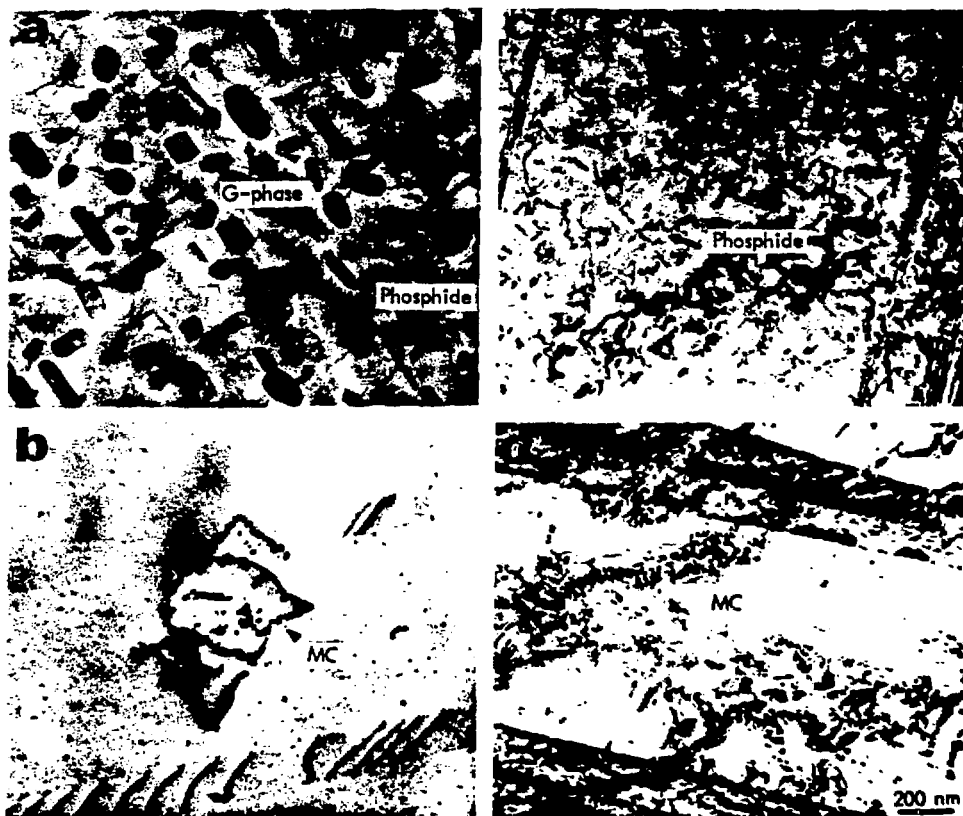

FIGURE 3

Alloy A7 irradiated with 4 MeV Ni-ions at 675°C with 0.4 appm He/dpa. (a) SA A7 (90 dpa), (b) beyond damage region of (a), (c) CW A7 (35 dpa), and (d) beyond damage region of (c).

However, a photographic enlargement was adequate to show the existence of phosphide particle interfacial bubbles >3 nm diameter (inset of Fig. 2b). A distribution of larger bubbles occurred at the G phase particle-matrix interfaces.

4. DISCUSSION

In the results presented above it was observed that cavity formation was absent when a high density of large phosphide precipitates formed during irradiation. This suggests that a large precipitate matrix interfacial area may be associated with swelling suppression and here we suggest a mechanism by which this may occur. It is based on the requirement that the occurrence of bias driven cavity swelling under these conditions requires as a prerequisite the accumulation of a critical number of gas atoms, n_g^*, in each cavity. Most of the cavities observed occur on the precipitate-matrix interfaces, and for a given irradiation condition we conjecture, based on limited data,[3] a reasonably uniform cavity spacing per unit interfacial area. It follows, therefore, that in the high phosphorous alloy (Figure 1a) there are fewer gas atoms in each cavity than in the low phosphorous alloy (Figure 1b), by roughly the ratio of precipitate-matrix interfacial areas. As a consequence of this dilution we suggest that the accumulation of n_g^* gas atoms has not yet occurred in the high phosphorous alloy, while n_g^* has been exceeded in the low phosphorous alloy at the doses reported here. Theoretical calculations supporting this possibility are discussed below. The critical number of gas atoms n_g^* arises in calculations of the effect of gas on the critical radius for bias driven growth.

The theory of the critical cavity radius has been reviewed recently by Mansur and Coghlan.[7] The critical cavity radius arises as the larger of the two physical roots in the solution for cavity growth rate versus cavity radius. The other root describes a stable cavity radius where a cavity will remain without shrinkage or growth unless there is further gas accumulation. Cavity growth results when a net vacancy influx occurs by excess vacancy over interstitial influx driven by cavity-dislocation bias, which is opposed by thermal vacancy emission. Thermal vacancy emission increases rapidly for smaller cavity sizes, such that there is some size at which the thermal vacancy outflux equals the excess vacancy over interstitial influx. The radius at which this occurs is termed the critical radius. However, internal gas pressure reduces thermal vacancy emission, and thus the critical radius occurs at smaller values when there is contained gas. The theory shows, however, that if there is enough contained gas the thermal vacancy outflux cannot ever exceed the excess vacancy influx. As the gas content in a cavity increases, a level, n_g^*, is reached where the critical radius abruptly drops to zero. Once a cavity of any size accumulates n_g^* gas atoms it definitely will grow by bias driven growth and need not wait for point defect flux fluctuations to carry it above a (gas content dependent) critical radius.

Figure 2(a) shows direct evidence cf fine bubbles on the phosphide-matrix interface in the high phosphorous alloy A7, which did not swell significantly during ion irradiation.

Table 1 summarizes the microstructural results for both neutron and ion irradiations and gives the number of gas atoms contained in cavities as estimated from the microstructural observations. The cavity densities in Table 1 are measured values for ion irradiation of alloy A7 where many small cavities were observed on precipitate-matrix interfaces, and neutron irradiation of alloy A7, where large cavities representing significant swelling were attached to precipitate-matrix interfaces. The

value for neutron irradiation of alloy A7 is estimated from the data for alloy A7, since no cavities were resolvable on the precipitate-matrix interfaces of alloy A7, because of poor specimen quality resulting from the high density of large precipitates. The number per unit volume of these cavities is obtained by assuming that each cavity is associated with the same specific precipitate-matrix interfacial area as in alloy A27. However, since the total precipitate matrix interfacial area in alloy A7 is nine times as large, the number of cavities per unit specimen volume is correspondingly nine times larger. Helium was generated at 0.4 appm/dpa in both types of irradiation. By assuming that all this helium is contained in the precipitate-matrix interfacial cavities we obtain the estimates of n_g given in the second last column of Table 1. These are upper limits, since some of the helium probably segregates to dislocations or resides in the matrix. However, relatively few visible bubbles are discerned on dislocations.

Theoretical calculations of n_g^* have also been made based on the methods of ref. [7], and are shown in the last column of Table 1. In these calculations the measured values of dislocation density were used, the cavity-matrix surface energy is taken as 1.5 J/nm, the vacancy migration and formation energies are 1.2 and 1.6 respectively, and the bias is 1%. These values are in the reasonable range for stainless steels, but no claim is made that they constitute a unique best fit. The theoretical results support the concept that the onset of bias-driven swelling occurs when n_g^* gas atoms are accumulated in the cavities. First, there is agreement between the magnitudes of the estimated values based on micro-structures and those theoretically calculated for neutron and ion conditions. Specifically, the critical number of gas atoms n_g^* is higher for the neutron case because 555°C is

a higher temperature with respect to 10^{-6} dpa/s than is 675°C with respect to ~3 × 10^{-3} dpa/s. Secondly, it is seen that n_g^* has not yet been achieved in the 50 dpa ion irradiated specimen A7 and therefore it is predicted that bias driven swelling is not yet possible. This is in agreement with the observation. In the neutron case it is calculated that n_g^* is below the number of helium atoms contained in a cavity in alloy A27 and hence it is predicted that bias driven swelling should be taking place. Again, this is in agreement with observation. In alloy A7, however, it is calculated that n_g^* is larger than the number of contained gas atoms and hence that bias driven swelling should not be occurring. Again this is consistent with the observed behavior.

This swelling suppression with increasing precipitate density is not unique but is observed frequently in many other alloy systems where profuse fine precipitates, such as γ, MC, or even oxide particles, preexist or are formed during irradiation. Brager and Garner[8] observed an extended incubation period for cavity nucleation in AISI 316 alloys neutron irradiated at temperatures ranging from 400 to 600°C as the silicon content was increased. This increase in silicon content was accompanied by formation of γ and other silicon and nickel-rich precipitates. Shaw et al.[9] reported that helium bubble size distributions are significantly refined by γ -particles in Al, Ti, and/or Si-doped nickel-base super-alloys. A strong association between MC particles and helium bubbles has been observed on many occasions in Ti-modified austenitic stainless steels; cavity formation was suppressed when the MC particle density was greater than 10^{22} m^3.[10,11,12] Singh[13] reported improved swelling resistance in aluminum-oxide-dispersed austenitic stainless steel. It has also been shown recently that other precipitates such as γ, MC, G, and Laves phase in

stainless steel also provide sites for the nucleation of cavities.[11] It is plausible that the same effect is operating in these cases. Thus the higher the precipitate-matrix interfacial area of any of these precipitates, the finer is the distribution of gas atoms, and the longer it takes to accumulate n_g^* gas atoms.

It is also expected that the increased precipitate-matrix interfacial area introduces more point defect traps in the high phosphorous alloy. The theory of point defect trapping and its effects on swelling has been developed recently[1] to make quantitative estimates possible. These traps would tend to suppress swelling more in the high phosphorous alloy. However, quantitative estimates of this suppression for the microstructural data reported here reveal that the increased interfacial trap density in the high phosphorous alloy is not sufficient to cause the large suppression of swelling observed even when the point defect-trap binding energy is very high.[2] Similarly the observed swelling suppression cannot be attributed to greater point defect trapping on phosphorous atoms in solution. In fact, estimates based on the observed volume fractions of phosphide precipitates in the matrix show that in the high phosphorous alloy there are actually fewer phosphorous atoms in solution than in the low phosphorous alloy. Grain boundaries may play some role in accounting for the difference. Finally, the effect of precipitates on the bias of dislocations is more difficult to assess. Careful examination of TEM micrographs indicates that dislocations often bow out between precipitates. Bowed segments indicate that the dislocations are not absorbing point defects with equal ease everywhere, but the overall bias change by such pinning is not known. Solute segregation on dislocations is expected to be less in alloy A7 again because of more precipitation. Therefore, solute poisoning of

dislocations cannot be the cause of the longer incubation period in the phosphide precipitate dominated alloy. Cold work introduces a high dislocation density and refines phosphide particles to a greater extent. The incubation period is thereby expected to be further increased.

The mechanism of formation and the stability of the phosphide phase is of considerable interest. The absence of the phosphide phase beyond the peak damage region in ion irradiated specimens clearly demonstrates that irradiation accelerates its formation. The eventual replacement of the phosphide phase by G phase at higher doses is a similar phenomenon to the replacement of the MC phase by G phase in low phosphorus steels as discussed recently.[11] Further work is in progress involving irradiation and thermal aging of a range of phosphorus containing alloys to investigate the precipitation of phosphide phases in systems also containing the MC, G, and Laves phases.

1. L.K. Mansur, M.R. Hayns, and E. H. Lee, Phase stability during irradiation, eds., J.R. Holland, L.K. Mansur, and D.I. Potter, AIME, 1981, p. 359.

2. A.D. Brailsford and L.K. Mansur, J. Nucl. Mater. 103&104 (1981) 1403.

3. E.H. Lee, A.F. Rowcliffe, and L.K. Mansur, J. Nucl. Mater. 103&104 (1981) 1475.

4. M.B. Lewis, N.H. Packan, G.F. Wells, and R.A. Buhl, Nucl. Instr. and Methods 167 (1979) 233.

5. E.H. Lee and A.F. Rowcliffe, Microstructural Science 7 (1979) 403.

6. E.H. Lee, P.J. Maziasz, and A.F. Rowcliffe, Phase stability during irradiation, eds., J.R. Holland, L.K. Mansur, and D.I. Potter, AIME, 1981, p. 191.

7. L.K. Mansur and W.A. Coghlan, J. Nucl. Mater., to be published.

8. H.R. Brager and F.A. Garner, Phase stability during irradiation, eds., J.R. Holland, L.K. Mansur, and D.I. Potter, AIME, 1981, p. 219.

7. L.K. Mansur and W.A. Coghlan, J. Nucl. Mater., to be published.

8. H.R. Brager and F.A. Garnaer, Phase stability during irradiation, eds., J.R. Holland, L.K. Mansur, and D.I. Potter, AIME, 1981, p. 219.

9. M.P. Shaw, B. Ralph, and W.M. Stobbs, J. Nucl. Mater. 115 (1983) p. 1.

10. P.J. Maziasz, Phase stability during irradiation, eds., J.R. Holland, L.K. Mansur, and D.I. Potter, AIME, 1981, p. 477.

11. A.F. Rowcliffe and E.H. Lee, J. Nucl. Mater. 108&109 (1982) p. 306.

12. E.H. Lee, N.H. Packan, and L.K. Mansur, J. Nucl. Mater. 117 (1983) p. 123.

13. B.N. Singh, Properties of Reactor Structural Alloys after Neutron or Particle Irradiation, ASTM STP 570 (1975) p. 543.

DISCLAIMER